

See discussions, stats, and author profiles for this publication at: <https://www.researchgate.net/publication/51633712>

# Detection of the H-1 and N-15 NMR Resonances of Sulfamate Groups in Aqueous Solution: A New Tool for Heparin and Heparan Sulfate Characterization

ARTICLE in ANALYTICAL CHEMISTRY · SEPTEMBER 2011

Impact Factor: 5.64 · DOI: 10.1021/ac202144m · Source: PubMed

---

CITATIONS

19

---

READS

44

## 3 AUTHORS:



Derek J Langeslay

BASF SE

13 PUBLICATIONS 149 CITATIONS

SEE PROFILE



Szabolcs Béni

Semmelweis University

73 PUBLICATIONS 695 CITATIONS

SEE PROFILE



Cynthia K Larive

University of California, Riverside

180 PUBLICATIONS 3,672 CITATIONS

SEE PROFILE

# Detection of the $^1\text{H}$ and $^{15}\text{N}$ NMR Resonances of Sulfamate Groups in Aqueous Solution: A New Tool for Heparin and Heparan Sulfate Characterization

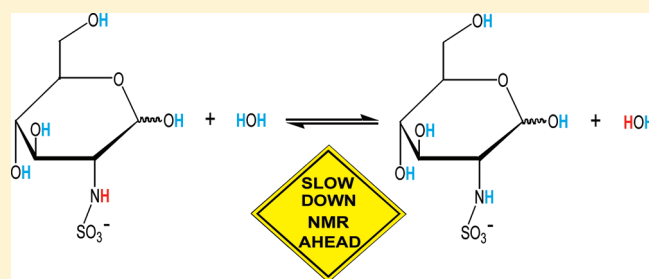
Derek J. Langeslay,<sup>†</sup> Szabolcs Beni,<sup>†,‡</sup> and Cynthia K. Larive<sup>\*,†</sup>

<sup>†</sup>Department of Chemistry, University of California—Riverside, Riverside, California 92521, United States

<sup>‡</sup>Semmelweis University, Department of Pharmaceutical Chemistry, Hógyes Endre u. 9, H-1092 Budapest, Hungary

 Supporting Information

**ABSTRACT:** Sulfamate ( $\text{NH}\text{SO}_3^-$ ) groups are critically important structural elements of the glycosaminoglycans heparin and heparan sulfate (HS). Experimental conditions are presented for detection of the sulfamate  $^1\text{H}$  NMR resonances in aqueous solution. NMR spectra reported for *N*-sulfoglucosamine (GlcNS) and the synthetic pentasaccharide drug fondaparinux demonstrate the broad utility of the sulfamate group  $^1\text{H}$  chemical shifts to reflect differences in molecular structure. The sulfamate protons also provide an efficient route for detection of  $^{15}\text{N}$  chemical shifts through proton–nitrogen correlations measured with the heteronuclear single quantum coherence (HSQC) experiment. The HSQC spectra of GlcNS, fondaparinux, and the low-molecular weight heparin enoxaparin illustrate the power of the  $^1\text{H}$  and  $^{15}\text{N}$  chemical shifts of the sulfamate NH groups for the structural characterization of heparin and HS.



Heparin, a potent and pharmaceutically important anticoagulant,<sup>1</sup> and the related glycosaminoglycan (GAG) heparan sulfate (HS) are involved in many critical biological processes including cell differentiation, development, and adhesion,<sup>2,3</sup> inflammation,<sup>4</sup> as well as pathological conditions including cancer and viral infections.<sup>5,6</sup> NMR has proved to be an invaluable method for characterizing heparin isolated from biological sources<sup>7–9</sup> as well as synthetic oligosaccharides<sup>10</sup> and analogues produced from related materials, for example, the *Escherichia coli* K5 bacterial capsular polysaccharide heparosan.<sup>11</sup> The value of NMR for the characterization of these types of materials was poignantly demonstrated by the contamination in 2008 of the pharmaceutical heparin supply chain with oversulfated chondroitin sulfate (OSCS).<sup>12–14</sup> NMR spectroscopy played a crucial role in determining the structure of the OCSC contaminant and in the screening of lots for pharmaceutical use.<sup>12,15–17</sup> Because heparin and HS mediate numerous biological processes through protein binding,<sup>18</sup> NMR is also crucial in revealing the nature of the molecular level interactions of these GAGs and their binding partners.<sup>19–21</sup> The work described herein extends the use of NMR for heparin characterization to allow, for the first time, spectroscopic measurement of the protons of the important heparin sulfamate ( $\text{NH}\text{SO}_3^-$ ) moieties in aqueous milieu and, through these protons, measurement of  $^{15}\text{N}$  chemical shifts at natural abundance. In addition to their presence in heparin and HS, sulfamates are also important moieties in many bioactive compounds such as the cyclamate class of sweeteners.<sup>22</sup> The chemistry of sulfamates, including their protonation equilibria, has been summarized by Benson and Spillane.<sup>23</sup>

Heparin and heparan sulfate are structurally diverse sulfonated linear polysaccharides consisting of  $1 \rightarrow 4$  linked repeating disaccharide subunits containing  $\alpha$ -L-iduronic (IdoA) or  $\beta$ -D-glucuronic acid (GlcA) and glucosamine (GlcN). The glucosamine residue may be unmodified, *N*-sulfonated (GlcNS), or *N*-acetylated (GlcNAc) and can contain variable patterns of *O*-sulfonation at the 3-O and 6-O positions.<sup>24</sup> The major disaccharide sequence of heparin is the trisulfonated L-IdoA(2S)-D-GlcNS-(6S), which comprises over 70% of heparin isolated from porcine intestinal mucosa; however, there is significant structural variability along the heparin chain which is important for its biological functions.<sup>25</sup> The sulfonate content of HS is lower than heparin with a GlcNAc to GlcNS ratio above 3, while HS has about twice the level of glucuronic as iduronic acid.<sup>26</sup>

Characterization of the intact heparin and HS biopolymers is complicated by their inherent complexity due to both structural microheterogeneity and polydispersity.<sup>27</sup> Despite this complexity, [ $^1\text{H}$ ,  $^{13}\text{C}$ ] heteronuclear single quantum coherence (HSQC) NMR spectra provide useful information about heparin structural features and substitution patterns.<sup>28</sup> Nitrogen-15 NMR has proved less useful at natural abundance levels, although strategies to enrich the abundance of this nucleus in bacterial or mammalian cell culture have demonstrated the value of [ $^1\text{H}$ ,  $^{15}\text{N}$ ]HSQC spectra for GAG characterization.<sup>11,29</sup> Previous studies using  $^{15}\text{N}$  NMR have been largely limited to characterization of GlcNAc

**Received:** August 14, 2011

**Accepted:** September 13, 2011

**Published:** September 13, 2011

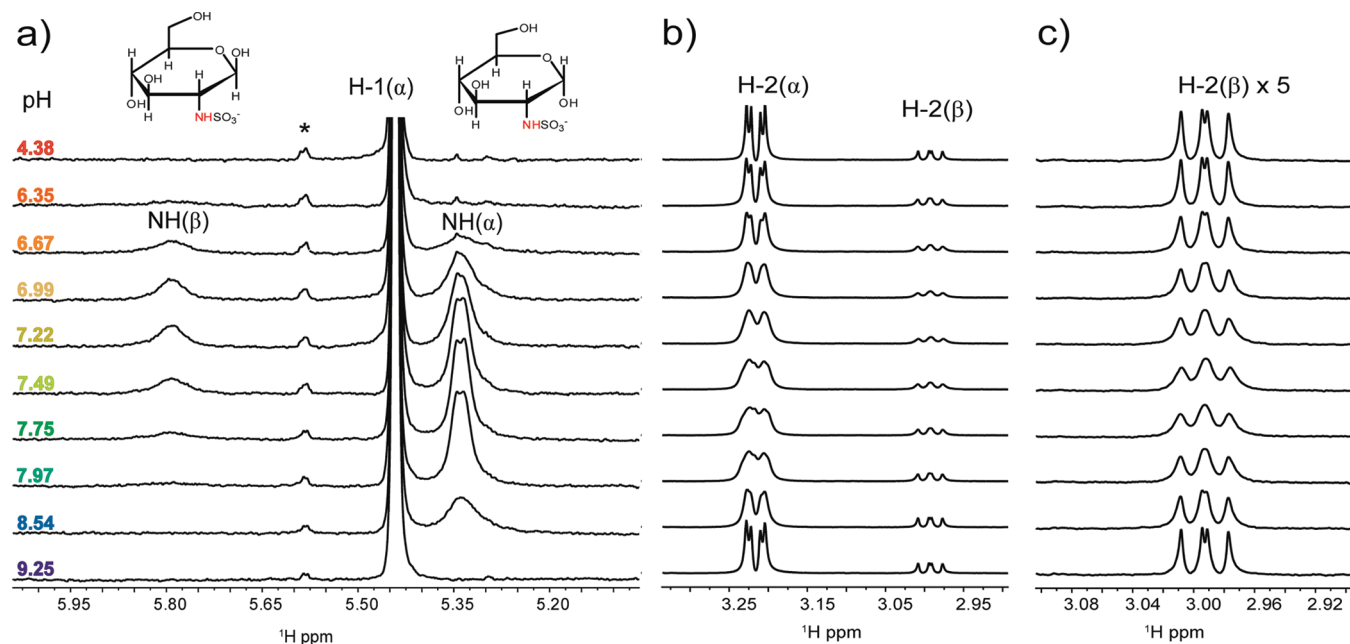


**Figure 1.** Selected regions of the  $^1\text{H}$  NMR spectra of *N*-sulfo-D-glucosamine (GlcNS) measured as a function of pH in 90%  $\text{H}_2\text{O}$ /10%  $\text{D}_2\text{O}$  at 25  $^\circ\text{C}$  using WATERGATE W5 solvent suppression. (a) The sulfamate proton resonances of the GlcNS  $\alpha$  (5.34 ppm) and  $\beta$  (5.79 ppm) anomers. The \* marks the carbon-bound proton resonance of an impurity. (b) The spectral region containing the GlcNS H-2 resonances showing the effect of the sulfamate proton chemical exchange. (c) A 5-fold scale enhancement of the H-2 resonance of the  $\beta$  anomer.

residues prevalent in chondroitin sulfate, dermatan sulfate, HS, and hyaluronic acid,<sup>29,30</sup> and present in much lower amounts in heparin. To our knowledge  $[\text{H},^{15}\text{N}]$ HSQC spectra have not been previously reported for heparin characterization, even for the GlcNAc residues. Like the backbone amide protons of peptides and proteins, the nitrogen-bound protons of GlcNAc exchange slowly with water in aqueous solution due to the partial double-bond character of the amide bond.<sup>29,31,32</sup> As a result, these amide protons give rise to sharp resonances easily detectable in the  $^1\text{H}$  NMR spectra of GAGs measured in aqueous solution, even when presaturation is used for suppression of the solvent resonance. In contrast, the sulfamate protons of the structurally and biologically important GlcNS residues have not been used for the NMR characterization of heparin and HS, most likely because of their fast exchange with water. We were able to find a single reference to detection of a weak  $\text{NH}\text{SO}_3^-$  cross peak in a  $[\text{H},^{15}\text{N}]$ HSQC spectrum of  $^{13}\text{C}$  and  $^{15}\text{N}$ -labeled heparosan presented in the supporting materials of a report by Zhang et al.<sup>11</sup> This observation raises the question of whether it is possible to identify solution conditions in which the solvent exchange of the GlcNS sulfamate protons is sufficiently slow to permit their routine and reliable detection by  $^1\text{H}$  NMR.

## EXPERIMENTAL SECTION

**Materials and Reagents.** *N*-sulfolglucosamine and the NMR chemical shift reference standard 4,4-dimethyl-4-silapentane-1-sulfonic acid- $d_6$  (DSS) were purchased from the Sigma Chemical Company (St. Louis, MO). Fondaparinux sodium (trade name Arixtra) was obtained from the University Pharmacy and Department of Pharmacy Administration of Semmelweis University, formulated as prefilled syringes for clinical use. The Fondaparinux solutions were pooled, desalted on a 1.6 cm  $\times$  70 cm Sephadex G10 superfine column (GE Healthcare, Pittsburgh, PA) using

HPLC grade water (Honeywell Burdick & Jackson) as the eluent with a flow rate of 0.15 mL/min. Desalted Fondaparinux was lyophilized and stored at  $-20$   $^\circ\text{C}$  until analyzed. Enoxaparin sodium was purchased from the U.S. Pharmacopeia (USP, Rockville, MD). All samples were prepared in a solution containing 90%  $\text{H}_2\text{O}$  (HPLC grade) and 10%  $\text{D}_2\text{O}$  (Sigma) in phosphate buffer (Fisher Scientific, Pittsburgh, PA). Solution pH was adjusted using DCl and NaOD (Sigma) also dissolved in 90%  $\text{H}_2\text{O}$ /10%  $\text{D}_2\text{O}$ . The pH meter was calibrated with aqueous buffers (Fisher), and values are reported without correction for the deuterium isotope effect.

**NMR Experimental Parameters.** The  $^1\text{H}$  NMR spectra of GlcNS measured as a function of pH were collected using WATERGATE W5 solvent suppression (zgpgw5) into 65 536 complex data points using a 7183 Hz spectral window.<sup>33</sup> The WATERGATE delay of 121  $\mu\text{s}$  was optimized for the detection of the sulfamate  $^1\text{H}$  resonances. A Bruker Avance NMR spectrometer operating at 599.79 MHz and equipped with a broadband inverse (BBI) probe was used for these measurements. The spectra were acquired using a  $90^\circ$  pulse with a length of 8.55  $\mu\text{s}$  and a 2.0 s relaxation delay. Prior to Fourier transformation, the free induction decays (FIDs) were zero-filled to 65 536 points and apodized by multiplication with an exponential function equivalent to a line broadening of 4.0 Hz for the sulfamate region or 0.7 Hz for the spectral region containing the carbon-bound H-2 resonances.

The  $[\text{H},^{15}\text{N}]$ HSQC spectrum of GlcNS was acquired with the Bruker pulse sequence hsqcgpph using States-TPPI.<sup>34,35</sup> The spectrum was acquired into 4096 complex points in  $t_2$  with 128 scans coadded at each of the 160  $t_1$  increments. A 2 s relaxation delay was used, and an optimized sulfamate  $^1\text{J}_{\text{N-H}}$  of 80 Hz was determined by acquisition of an  $[\text{H},^{15}\text{N}]$ HSQC spectrum of GlcNS without  $^{15}\text{N}$  decoupling. Spectral windows of 6613 Hz in  $F_2$  and 1519 Hz in  $F_1$  were employed. Pulse lengths for the  $^1\text{H}$  and  $^{15}\text{N}$   $90^\circ$  pulses were 8.63  $\mu\text{s}$  at  $-5$  dB and 50  $\mu\text{s}$  at  $-4$  dB,

respectively.  $^{15}\text{N}$  GARP decoupling during acquisition used a  $200\ \mu\text{s}$   $^{15}\text{N}$  pulse at 10 dB. The spectrum was zero-filled to  $4096 \times 512$  data points and apodized using a cosine<sup>2</sup> window function. The  $^1\text{H}$  spectrum shown at the top of the contour plot was collected in one scan with the single pulse (zg) experiment using a  $90^\circ$  pulse of  $8.63\ \mu\text{s}$  at  $-5\ \text{dB}$  and a 2 s relaxation delay. Prior to Fourier transformation, the FID was zero-filled to 65 536 data points and multiplied by an exponential function equivalent to 0.5 Hz line broadening.  $^1\text{H}$  and  $^{15}\text{N}$  chemical shifts are referenced relative to DSS, which has a  $^1\text{H}$  chemical shift of 0.00 ppm.

The  $[^1\text{H}, ^{15}\text{N}]$ HSQC spectrum of fondaparinux was measured as described above for GlcNS except that 256 scans were coadded at each of 100  $t_1$  increments. Pulse lengths for the  $^1\text{H}$  and  $^{15}\text{N}$   $90^\circ$  pulses were  $9.85\ \mu\text{s}$  at  $-5\ \text{dB}$  and  $50\ \mu\text{s}$  at  $-4\ \text{dB}$ , respectively. The data were zero-filled to  $8192 \times 512$  points with linear prediction employed in  $F_1$ . Apodization using a cosine<sup>2</sup> window function preceded Fourier transformation. The WATERGATE W5 (zgpgw5) spectrum of fondaparinux is plotted along the top of the contour plot. The WATERGATE delay of  $300\ \mu\text{s}$  was optimized for the detection of the sulfamate  $^1\text{H}$  resonances. A total of 32 scans were acquired into 32 768 complex data points using a spectral window of 6613 Hz and a 10.0 s relaxation delay. Prior to Fourier transformation, the FID was zero-filled to 65 536 data points and multiplied by an exponential function equivalent to 0.5 Hz line broadening.

The  $[^1\text{H}-^{15}\text{N}]$ HSQC spectrum of enoxaparin sodium was measured using a Bruker Avance NMR spectrometer operating at 600.13 MHz and equipped with a triple resonance inverse (TXI) probe. Most acquisition parameters were the same as described above for GlcNS except that 288 scans were coadded at each of the 120  $t_1$  increments, a relaxation delay of 1.5 s, and a  $F_1$  spectral window of 2432 Hz were used. Pulse lengths for the  $^1\text{H}$  and  $^{15}\text{N}$   $90^\circ$  pulses were  $10.00\ \mu\text{s}$  at  $-4\ \text{dB}$  and  $39\ \mu\text{s}$  at  $-4.4\ \text{dB}$ , respectively. The data were zero-filled to  $8192 \times 512$  points and apodized by multiplication with a cosine<sup>2</sup> window function prior to Fourier transformation. The WATERGATE W5 spectra plotted above the contour plots were acquired with a WATERGATE delay of  $121\ \mu\text{s}$  for detection of the sulfamate resonances and the N-acetyl region of the spectrum. The  $^1\text{H}$  NMR spectra were acquired into 32 768 data points by coaddition of 16 (sulfamate resonances) or 128 (N-acetyl resonances) scans using a spectral window of 6613 Hz and a 2.0 s relaxation delay. The  $90^\circ$   $^1\text{H}$  pulse was calibrated as  $10.50\ \mu\text{s}$  at  $-5\ \text{dB}$ . Prior to Fourier transformation, the FID was zero-filled to 65 536 data points and multiplied by an exponential function equivalent to 0.5 Hz line broadening. The full  $[^1\text{H}-^{15}\text{N}]$ HSQC spectrum of enoxaparin sodium is presented in the Supporting Information as Figure S-1.

## RESULTS

We addressed the challenge of detecting the sulfamate protons by building on the large body of work involving NMR measurements of the amide protons of peptides and proteins and the nitrogen-bound protons of nucleotide bases, the building blocks of DNA and RNA. The exchange rates of these classes of NH protons are highly pH dependent. pH optima of 3–4 for detection of peptide backbone amide protons and pyrimidine nucleotides and 6–8 for purine nucleotides have been identified.<sup>36</sup> Shown in Figure 1 is the pH dependence of the  $^1\text{H}$  NMR spectrum of 5 mM GlcNS measured in 90%  $\text{H}_2\text{O}/10\% \text{D}_2\text{O}$  at  $25\ ^\circ\text{C}$  using WATERGATE W5 solvent suppression.<sup>28</sup> GlcNS is present in solution in both the  $\alpha$  and  $\beta$  anomeric forms, which

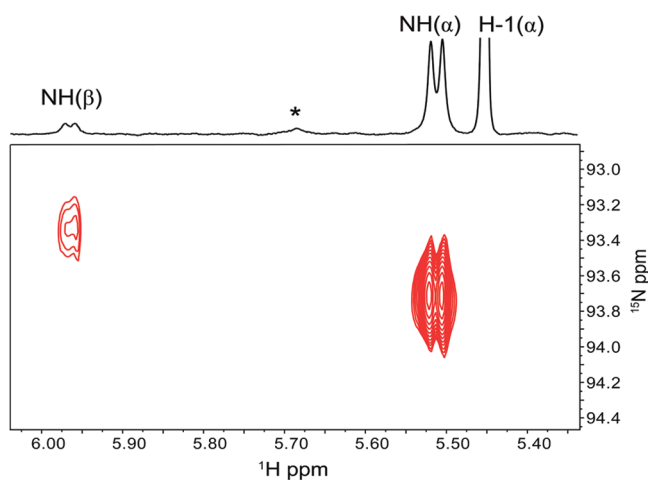


**Figure 2.**  $[^1\text{H}, ^{15}\text{N}]$  HSQC spectrum of GlcNS at pH 7.5 and  $5\ ^\circ\text{C}$ . The \* marks the carbon-bound proton resonance of an impurity.

appear from Figure 1a to have minima in their exchange rates at slightly different pH values. The assignment of the  $\alpha$  (5.34 ppm) and  $\beta$  (5.79 ppm) sulfamate group  $^1\text{H}$  resonances was based on their relative intensities, which are consistent with those of the carbon-bound anomeric H-1 resonances. At pH 7.49, the exchange rate of the sulfamate proton is sufficiently slow that the NH resonance of the  $\alpha$  anomer reflects the coupling to the adjacent GlcNS H-2. The rate of NH chemical exchange also has a pronounced effect on the peak width of the adjacent H-2 resonances as can be discerned by examination of Figure 1b,c. Below pH 6 and above pH 9 where the rate of exchange of the sulfamate protons with water is rapid, the H-2 resonances are sharp. At pH values where the exchange rate begins to slow and a broad NH resonance is detected, broadening can also be seen for the coupled H-2 resonances. For the  $\alpha$  anomer, the H-2 resonance at the exchange rate minimum (pH 7.5) is consistent with that of a complex multiplet including the NH coupling of 6 Hz. At this temperature, the  $\beta$  anomer sulfamate resonance never sharpens sufficiently to resolve its coupling to H-2.

With solution conditions in place to detect the sulfamate  $^1\text{H}$  NMR resonances, indirect detection of  $^{15}\text{N}$  chemical shifts via the HSQC NMR experiment becomes feasible.<sup>29,30</sup> Figure 2 shows the  $[^1\text{H}, ^{15}\text{N}]$ HSQC spectrum measured at  $5\ ^\circ\text{C}$  for 5 mg of GlcNS in  $40\ \mu\text{L}$  of 90%  $\text{H}_2\text{O}/10\% \text{D}_2\text{O}$ , 50 mM phosphate buffer, pH 7.5 using a 1.7 mm o.d. coaxial insert NMR tube. An average  $J_{\text{N-H}}$  of 80 Hz was used, and 160  $t_1$  increments were acquired. Reducing the temperature to  $5\ ^\circ\text{C}$  reduces the rate of NH– $\text{H}_2\text{O}$  exchange, sharpening the sulfamate proton resonances of both GlcNS anomers. The different chemical shifts of the  $^{15}\text{N}$  nuclei ( $\alpha = 93.71\ \text{ppm}$ ,  $\beta = 93.32\ \text{ppm}$ ) shown in Figure 2 are consistent with the values we reported previously using long-range  $^{15}\text{N}$ – $^1\text{H}$  couplings measured with the  $[^1\text{H}, ^{15}\text{N}]$  heteronuclear multiple-bond coherence (HMBC) experiment using carbon-bound protons and confirms the  $^1\text{H}$  resonance assignments of the two GlcNS anomers.<sup>37</sup>

Although detection of the GlcNS sulfamate  $^1\text{H}$  and  $^{15}\text{N}$  resonances is interesting, to be useful for GAG characterization the  $^1\text{H}$  and/or  $^{15}\text{N}$  NMR chemical shifts must be sensitive to subtle structural differences. We selected the synthetic heparin mimic fondaparinux to probe the potential value of  $[^1\text{H}, ^{15}\text{N}]$ -HSQC NMR spectra for heparin and HS structural characterization. The structure of fondaparinux is closely related to the native



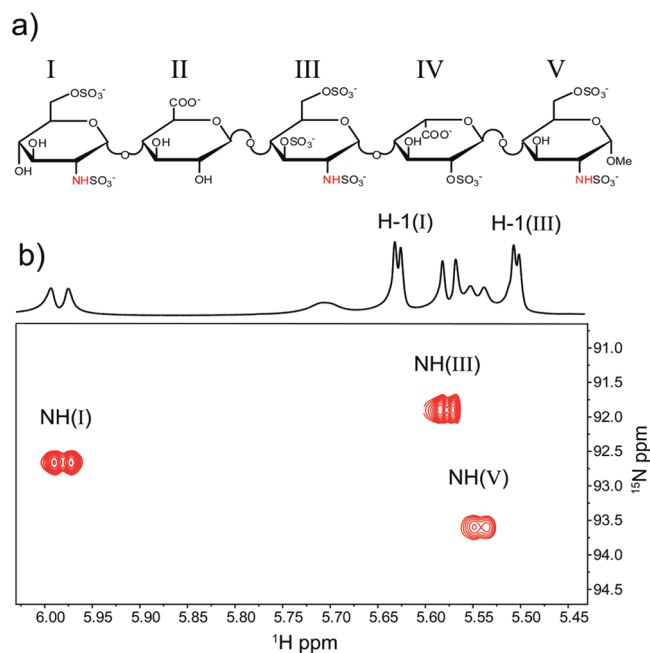


**Figure 3.** (a) Structure of the synthetic pentasaccharide fondaparinux, sodium ions omitted. The component monosaccharides are labeled I–V starting at the nonreducing end. (b)  $[^1\text{H}, ^{15}\text{N}]$ HSQC spectrum of fondaparinux in 90%  $\text{H}_2\text{O}/10\%$   $\text{D}_2\text{O}$  in 20 mM phosphate buffer at pH 8.2 and 5 °C. The  $^1\text{H}$  WATERGATE W5 spectrum is plotted at the top of the contour map showing the carbon-bound anomeric proton resonances of GlcNS residues I and III in addition to the sulfamate proton resonances.

heparin pentasaccharide responsible for binding to antithrombin III.<sup>38</sup> Fondaparinux is used clinically for treatment of thrombosis and marketed under the trade name Arixtra (GalaxoSmithKline).<sup>10</sup> The fondaparinux pentasaccharide contains three distinct sulfamate groups all in different chemical environments, as shown by the structure in Figure 3a. To our knowledge, neither the  $^1\text{H}$  nor  $^{15}\text{N}$  NMR chemical shifts of the fondaparinux sulfamate groups have been previously reported. From a series of  $^1\text{H}$  NMR survey spectra measured using WATERGATE W5 solvent suppression as a function of pH, similar to those shown in Figure 1, we determined a pH optimum of 8.2 for detection of the  $\text{NHOSO}_3^-$  protons of fondaparinux. The  $[^1\text{H}, ^{15}\text{N}]$ HSQC spectrum measured for 40 mM fondaparinux in 90%  $\text{H}_2\text{O}/10\%$   $\text{D}_2\text{O}$ , 20 mM phosphate buffer at pH 8.2 and 5 °C is shown in Figure 3b. Fondaparinux sulfamate group  $^1\text{H}$  resonance assignments were made using connectivities in the correlation spectroscopy (COSY), total correlation spectroscopy (TOCSY), and rotating-frame Overhauser effect spectroscopy (ROESY) spectra (Figures S-2, S-3, and S-4 in the Supporting Information, respectively). Each of the sulfamate  $^1\text{H}$  and  $^{15}\text{N}$  resonances of fondaparinux has a unique chemical shift. Starting with the first residue of the nonreducing end GlcNS(6S), we observe  $^1\text{H}$  and  $^{15}\text{N}$  chemical shifts of 5.99 and 92.66 ppm, respectively. This ring is connected through a  $1 \rightarrow 4$  linkage to an unsulfonated glucuronic acid residue. The chemical shifts of the  $^1\text{H}$  (5.58 ppm) and  $^{15}\text{N}$  (91.90 ppm) nuclei of the third residue, GlcNS(3S)(6S), may reflect the unique 3-O-sulfonation of this residue and its  $1 \rightarrow 4$  linkage to a 2-O-sulfonated iduronic acid residue. Finally, distinct  $^1\text{H}$  (5.55 ppm) and  $^{15}\text{N}$  (93.59 ppm) chemical shifts are also observed for the terminal GlcNS(6S)OMe residue. O-Methylation of the

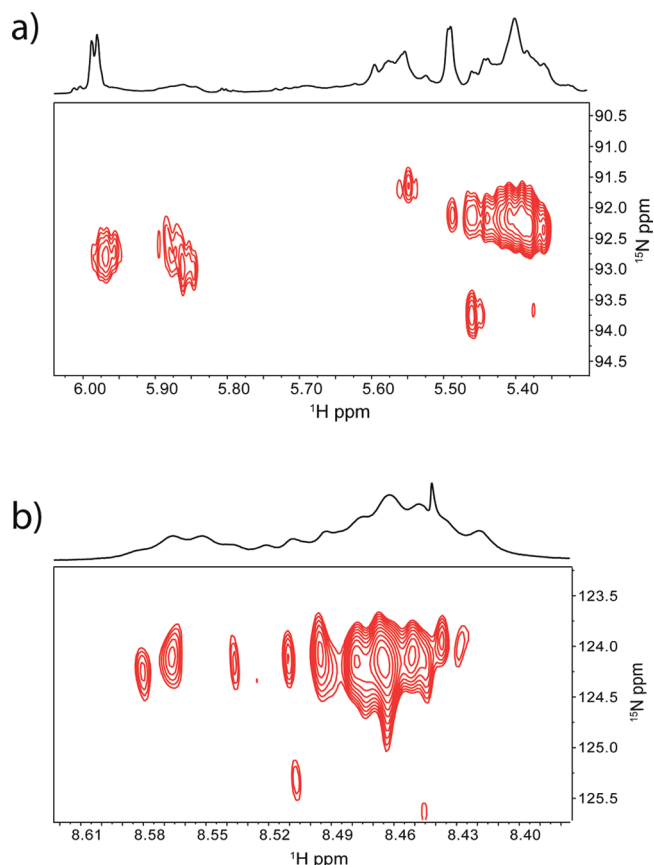


**Figure 4.**  $[^1\text{H}, ^{15}\text{N}]$  HSQC spectrum of enoxaparin sodium (USP) in 90%  $\text{H}_2\text{O}$  and 10%  $\text{D}_2\text{O}$  20 mM phosphate buffer at pH 8.2 and 5 °C. (a) Expansion of the spectral region showing the correlations for the sulfamate protons. (b) Expansion of the N-acetyl region of the HSQC spectrum at a higher scale enhancement. A  $^1\text{H}$  WATERGATE W5 spectrum is plotted at the top of the contour maps. The full HSQC spectrum is presented in Figure S-1 in the Supporting Information.

fondaparinux reducing end anomeric OH group prevents mutarotation, simplifying the NMR spectrum. The results in Figure 3 indicate that both the  $^1\text{H}$  and  $^{15}\text{N}$  chemical shifts of the sulfamate groups can report on the local environment of an individual GlcNS residue, consistent with similar observations for the amide resonances of GlcNAc residues in other GAGs.<sup>11,29,30</sup>

Stable isotope labeling with  $^{15}\text{N}$ -glutamine in cell culture has greatly facilitated the NMR characterization of the GAGs hyaluronic acid, chondroitin sulfate, and dermatan sulfate.<sup>29,30</sup> Although *E. coli* K5 was systematically modified to generate chemoenzymatically-synthesized heparin which was also extensively characterized by NMR,<sup>11</sup> heparin isolated from biological sources has yet to be produced in a stable isotope labeled form. The sensitivity of the  $[^1\text{H}, ^{15}\text{N}]$ HSQC spectra measured for GlcNS (Figure 2) and fondaparinux (Figure 3b) suggest that it should be possible to measure similar spectra for pharmaceutical heparin, even at natural abundance levels of  $^{15}\text{N}$ . Figure 4a shows the sulfamate region of the  $[^1\text{H}, ^{15}\text{N}]$ HSQC spectrum measured for a 75 mg/mL solution of the low-molecular weight heparin drug enoxaparin sodium (USP) in 90%  $\text{H}_2\text{O}/10\%$   $\text{D}_2\text{O}$ , 20 mM phosphate buffer, pH 8.2 at 5 °C. Enoxaparin is produced through  $\beta$ -elimination of a heparin benzyl ester and has a weight-average molecular weight of 4500 Da. Because enoxaparin is a complicated mixture of heparin oligosaccharides, the complex pattern of

$^1\text{H}$  and  $^{15}\text{N}$  cross peaks observed in Figure 4a is not surprising. Figure 4b shows the expansion of the N-acetyl region of the enoxaparin [ $^1\text{H}$ ,  $^{15}\text{N}$ ]HSQC spectrum. In addition to detection of the sulfamate NH groups, we also observe a weaker set of HSQC cross peaks for the GlcNAc amide groups, even though the solution pH is not at the optimum value for detection of these protons. Although the N-acetyl peaks are less intense than those of the sulfamate NH groups because of the low abundance of GlcNAc residues in heparin, the amide NH cross peaks are easily detected even at natural abundance levels of  $^{15}\text{N}$ .

Interpretation of the  $^1\text{H}$  and  $^{15}\text{N}$  chemical shifts of a complex material like enoxaparin is beyond the scope of the current work and will likely require detailed analysis of isolated oligosaccharides to assemble a library of sulfamate NH chemical shifts, as are currently available to facilitate interpretation of heparin [ $^1\text{H}$ ,  $^{13}\text{C}$ ]HSQC spectra.<sup>28</sup> However, even without a detailed molecular-level analysis, Figure 4 demonstrates the potential of the [ $^1\text{H}$ ,  $^{15}\text{N}$ ]HSQC spectrum as a novel fingerprint for the quality assurance of pharmaceutical heparin. In addition to the use of sulfamate  $^1\text{H}$  and  $^{15}\text{N}$  NMR chemical shifts for structural characterization, their direct detection in aqueous solution should provide new insights into the molecular-level interactions important in heparin–protein binding.

## ■ ASSOCIATED CONTENT

**S Supporting Information.** Additional information as noted in text. This material is available free of charge via the Internet at <http://pubs.acs.org>.

## ■ AUTHOR INFORMATION

### Corresponding Author

\*E-mail: [clarive@ucr.edu](mailto:clarive@ucr.edu).

## ■ ACKNOWLEDGMENT

C.K.L. gratefully acknowledges funding from the National Science Foundation through Grant No. CHE-0848976 and the Mizutani Foundation for Glycoscience. Sz.B. gratefully acknowledges support from KTIA-OTKA Grant MB08A/80066. The authors thank D. L. Rabenstein and L. J. Mueller for helpful discussions of this work.

## ■ REFERENCES

- (1) Mousa, S. A. *Semin. Thromb. Hemostasis* **2007**, *33*, 524–533.
- (2) Whitelock, J. M.; Iozzo, R. V. *Chem. Rev.* **2005**, *105*, 2745–2764.
- (3) Krees, H.; Schönherr, E. *J. Cell. Physiol.* **2001**, *189*, 266–274.
- (4) Li, J.-p.; Vlodavsk, I. *Thromb. Haemostasis* **2009**, *102*, 823–828.
- (5) Raman, R.; Sasisekharan, V.; Sasisekharan, R. *Chem. Biol.* **2005**, *12*, 267–277.
- (6) Götte, M.; Yip, G. W. *Cancer Res.* **2006**, *66*, 10233–10237.
- (7) Rudd, T. R.; Skidmore, M. A.; Guimond, S. E.; Cosentino, C.; Torri, G.; Fernig, D. G.; Lauder, R. M.; Guerrini, M.; Yates, E. A. *Glycobiology* **2009**, *19*, 52–56.
- (8) Limtiaco, J. F. K.; Beni, Sz.; Jones, C. J.; Langeslay, D. J.; Larive, C. K. *Carbohydr. Res.* **2011**, *346*, 2244–2254.
- (9) Korir, A. K.; Larive, C. K. *Anal. Bioanal. Chem.* **2009**, *393*, 155–169.
- (10) De Kort, M.; Buijsman, R. C.; van Boeckel, C. A. A. *Drug Discovery Today* **2005**, *10*, 769–779.
- (11) Zhang, Z.; McCallum, S. A.; Xie, J.; Nieto, L.; Corzana, F.; Jiménez-Barbero, J.; Chen, M.; Liu, J.; Linhardt, R. J. *J. Am. Chem. Soc.* **2008**, *130*, 12998–13007.
- (12) Guerrini, M.; Beccati, D.; Shriver, Z.; Naggi, A.; Viswanathan, K.; Bisio, A.; Capila, I.; Lansing, J. C.; Guglieri, S.; Fraser, B.; Al-Hakim, A.; Gunay, N. S.; Zhang, Z. Q.; Robinson, L.; Buhse, L.; Nasr, M.; Woodcock, J.; Langer, R.; Venkataraman, G.; Linhardt, R. J.; Casu, B.; Torri, G.; Sasisekharan, R. *Nat. Biotechnol.* **2008**, *26*, 669–675.
- (13) Kishimoto, T. K.; Viswanathan, K.; Ganguly, T.; Elankumaran, S.; Smith, S.; Pelzer, K.; Lansing, J. C.; Sriranganathan, N.; Zhao, G. L.; Galcheva-Gargova, Z.; Al-Hakim, A.; Bailey, G. S.; Fraser, B.; Roy, S.; Rogers-Cotrone, T.; Buhse, L.; Whary, M.; Fox, J.; Nasr, M.; Dal Pan, G. J.; Shriver, Z.; Langer, R. S.; Venkataraman, G.; Austen, K. F.; Woodcock, J.; Sasisekharan, R. *N. Engl. J. Med.* **2008**, *358*, 2457–2467.
- (14) Blossom, D. B.; Kallen, A. J.; Patel, P. R.; Elward, A.; Robinson, L.; Gao, G. P.; Langer, R.; Perkins, K. M.; Jaeger, J. L.; Kurkjian, K. M.; Jones, M.; Schillie, S. F.; Shehab, N.; Ketterer, D.; Venkataraman, G.; Kishimoto, T. K.; Shriver, Z.; McMahon, A. W.; Austen, K. F.; Kozlowski, S.; Srinivasan, A.; Turabelidze, G.; Gould, C. V.; Arduino, M. J.; Sasisekharan, R. *N. Engl. J. Med.* **2008**, *359*, 2674–2684.
- (15) Zhang, Z.; Weiwer, M.; Li, B.; Kemp, M. M.; Daman, T. H.; Linhardt, R. J. *J. Med. Chem.* **2008**, *51*, 5498–5501.
- (16) Guerrini, M.; Zhang, Z.; Shriver, Z.; Naggi, A.; Masuko, S.; Langer, R.; Casu, B.; Linhardt, R. J.; Torri, G.; Sasisekharan, R. *Proc. Natl. Acad. Sci. U.S.A.* **2009**, *106*, 16956–16961.
- (17) Beni, Sz.; Limtiaco, J. F. K.; Larive, C. K. *Anal. Bioanal. Chem.* **2011**, *399*, 527–539.
- (18) Gandhi, N. S.; Macera, R. L. *Chem. Biol. Drug Des.* **2008**, *72*, 455–482.
- (19) Powell, A. K.; Yates, E. A.; Fernig, D. G.; Turnbull, J. E. *Glycobiology* **2004**, *14*, 17R–30R.
- (20) Capila, I.; Linhardt, R. J. *Angew. Chem., Int. Ed.* **2002**, *41*, 390–412.
- (21) Laguri, C.; Sapay, N.; Simorre, J.-P.; Brutscher, B.; Imberty, A.; Gans, P.; Lorat-Jacob, H. *J. Am. Chem. Soc.* **2011**, *133*, 9642–9645.
- (22) Spillane, W. J.; Ryder, C. A.; Walsh, R.; Curran, P. J.; Concagh, D. *Food Chem.* **1996**, *56*, 255–261.
- (23) Benson, G. A.; Spillane, W. J. *Chem. Rev.* **1980**, *80*, 151–186.
- (24) Rabenstein, D. L. *Nat. Prod. Rep.* **2002**, *19*, 312–331.
- (25) Gatti, G.; Casu, B.; Hamer, G. K.; Perlin, A. S. *Macromolecules* **1979**, *12*, 1001–1007.
- (26) Gallagher, J. T.; Walker, A. *Biochem. J.* **1985**, *230*, 665–674.
- (27) Jones, C. J.; Beni, Sz.; Limtiaco, J. F. K.; Langeslay, D. J.; Larive, C. K. *Annu. Rev. Anal. Chem.* **2011**, *4*, 439–465.
- (28) Guerrini, M.; Naggi, A.; Guglieri, S.; Santarsiero, R.; Torri, G. *Anal. Biochem.* **2005**, *337*, 35–47.
- (29) Pomin, V. H.; Sharp, J. S.; Li, X.; Wang, L.; Prestegard, J. H. *Anal. Chem.* **2010**, *82*, 4078–4088.
- (30) Blundell, C. D.; DeAngelis, P. L.; Day, A. J.; Almond, A. *Glycobiology* **2004**, *14*, 999–1009.
- (31) Pauling, L.; Corey, R. B. *Proc. Natl. Acad. Sci. U.S.A.* **1951**, *37*, 729–740.
- (32) Almond, A.; DeAngelis, P. L.; Blundell, C. D. *J. Am. Chem. Soc.* **2005**, *127*, 1086–1087.
- (33) Liu, M. L.; Mao, X. A.; Ye, C. H.; Huang, H.; Nicolson, J. C. *J. Magn. Reson.* **1998**, *132*, 125–129.
- (34) Bodenhausen, G.; Ruben, D. J. *Chem. Phys. Lett.* **1980**, *69*, 185–189.
- (35) Ruiz-Cabello, J.; Vuister, G. W.; Moonen, C. T. W.; van Gelderen, P.; Cohen, J.; van Zijl, P. C. M. *Magn. Reson. Imaging* **1992**, *100*, 282–302.
- (36) Bai, Y.; Englander, J. L.; Mayne, L.; Milne, J. S.; Englander, W. S. *Method Enzymol.* **1995**, *259*, 344–356.
- (37) Limtiaco, J. F.; Langeslay, D. J.; Beni, Sz.; Larive, C. K. *J. Magn. Reson.* **2011**, *209*, 323–331.
- (38) Atha, D. A.; Stephens, A. W.; Rosenberg, R. D. *Proc. Natl. Acad. Sci. U.S.A.* **1984**, *81*, 1030–1034.